Influence of surfactant structure on reverse micelle size and charge for non-polar electrophoretic inks

Mary E. Parent, Jun Yang, Yoocharn Jeon, Michael F. Toney, Zhang-Lin Zhou, Dick Henze

HP Laboratories
HPL-2011-110

Keyword(s):

reverse micelles; non-polar media; transient current; small-angle x-ray scattering; electrophoretic displays

Abstract:

Electrophoretic inks, which are suspensions of colorant particles that are controllably concentrated and dispersed by applied electric fields, are the leading commercial technology for high quality reflective displays. Extending the state-of-the-art for high fidelity color in these displays requires improved understanding and control of the colloidal systems. In these inks, reverse micelles in non-polar media play key roles in media and particle charging. Here we investigate the effect of surfactant structure on reverse micelle size and charging properties by synthesizing different surfactants with variations in polyamine polar head groups. Small-angle x-ray scattering (SAXS) and dynamic light scattering (DLS) were used to determine micelle core plus shell size and micelle hydrodynamic radius, respectively. The results from SAXS agreed with DLS and showed that increasing polyamines in the surfactant head increased the micelle size. The hydrodynamic radius was also calculated based on transient current measurements, and agreed well with the DLS results. The transient current technique further determined that increasing polyamines increased the charge stabilization capability of the micelles and that an analogous commercial surfactant OLOA 11000 made for a lower concentration of charge generating ions in solution. Formulating magenta inks with the various surfactants showed that the absence of amine in the surfactant head was detrimental to particle stabilization and device performance.

External Posting Date: July 21, 2011 [Fulltext] Approved for External Publication
Internal Posting Date: July 21, 2011 [Fulltext]

Influence of surfactant structure on reverse micelle size and charge for non-polar electrophoretic inks

Mary E. Parent [a], Jun Yang [a], Yoocharn Jeon [a], Michael F. Toney [b], Zhang-Lin Zhou [a] *, and Dick Henze [a]

[a] HP Labs, Hewlett-Packard Co., 1501 Page Mill Road, Palo Alto, CA 94304, USA

[b] Stanford Synchrotron Radiation Lightsource, 2575 Sand Hill Road, Menlo Park, CA 94025

* Corresponding author, Phone- 650-857-2036, Fax- 650-857-8051, Email: zhang-lin.zhou@hp.com

For submission to Langmuir

July 12, 2011

Abstract

Electrophoretic inks, which are suspensions of colorant particles that are controllably concentrated and dispersed by applied electric fields, are the leading commercial technology for high quality reflective displays. Extending the state-of-the-art for high fidelity color in these displays requires improved understanding and control of the colloidal systems. In these inks, reverse micelles in non-polar media play key roles in media and particle charging. Here we investigate the effect of surfactant structure on reverse micelle size and charging properties by synthesizing different surfactants with variations in polyamine polar head groups. Small-angle x-ray scattering (SAXS) and dynamic light scattering (DLS) were used to determine micelle core plus shell size and micelle hydrodynamic radius, respectively. The results from SAXS agreed with DLS and showed that increasing polyamines in the surfactant head increased the micelle size. The hydrodynamic radius was also calculated based on transient current measurements, and agreed well with the DLS results. The transient current technique further determined that increasing polyamines increased the charge stabilization capability of the micelles and that an analogous commercial surfactant OLOA 11000 made for a lower concentration of charge generating ions in solution. Formulating magenta inks with the various surfactants showed that the absence of amine in the surfactant head was detrimental to particle stabilization and device performance.

Keywords: reverse micelles, non-polar media, transient current, small-angle x-ray scattering, electrophoretic displays

1. Introduction

Charge transport and particle charging in non-polar media are of interest in a variety of fields such as reflective displays[1,2] and drug delivery[3,4]. The state-of-the-art for reflective display technology is electrophoretic ink, which acts as the imaging fluid within display cells. It contains colloidal colorant particles suspended in non-polar media with surfactants that charge the particles and increase the conductivity of the non-polar media.[5] Unlike in aqueous solutions, opposite charges are difficult to separate in non-polar media, as evident by comparing relative permittivity (ε_r), for water $\varepsilon_r \approx 80$ and for non-polar solvents $\varepsilon_r \approx 2$ at room temperature. Considering the distance d of closest approach between two ions (Bjerrum length λ_B), where thermal energy k_BT overcomes coulombic attraction $E_{coul} = -e^2 / (4\pi\varepsilon_r\varepsilon_o d)$, λ_B is 0.7 nm for water and 28 nm for non-polar solvents.[5] Thus, for there to be dissociated ions in non-polar solvents, the ion-ion spacing must be about 40 times larger than in water. Non-polar media is therefore beneficial for reducing current flow and power consumption in reflective displays since conductivity is low. However, the imaging fluid functions via electrophoresis, so some stable charge is necessary.

Surfactants in non-polar media form reverse micelles once above a critical concentration.[6,7] The polar head group of the surfactants effectively increases the solution's relative permittivity, which locally reduces the large Bjerrum length significantly. The reverse micelles can therefore act as charge directors that are able to stabilize dissociated ions and play key roles in electrical conduction and colloidal particle charging.[5] Surfactants commonly studied in non-polar fluids are basic polyisobutylene (PIB) succinimide,[8-13] anionic sodium di-2-ethylhexyl-sulfosuccinate (AOT),[14-18] and acidic sorbitan oleate (SPAN).[19,20] Many of these studies show the effect of surfactant concentration on particle charging and also on solution conductivity.[9,10,15-18] Other researchers conduct more detailed analysis on the charge concentration of the suspending medium alone with varying surfactant concentration.[11-14] More recently, investigations compare surfactant chemistry and show there are common features to particle charging regardless of surfactant type.[21-23] However, these studies consider only gross differences in surfactant chemistry and focus on particle charge effects. In addition to the existing questions on the effect of small variations in surfactant structure on particle charging and charge concentration of the suspending medium, there are often questions of surfactant purity when using commercial surfactants.

In this study we investigate purified PIB succinimide surfactants synthesized with systematic variations in the polyamine polar head. Reverse micelle size and charge in non-polar solutions are determined with small-angle x-ray scattering, dynamic light scattering, and transient current measurements. Colorant particles are added to the surfactant solutions and electro-optical performance is evaluated in test devices. By investigating fundamental relationships between surfactant chemistry and reverse micelle and imaging fluid behavior, an improved understanding of electrophoretic colloidal systems is gained for improved color reflective display performance.

2. Materials and Methods

2.1. Surfactant syntheses and solutions. Polyamines ethylenediamine, diethylenetriamine, triethylenetetraamine, and tetraethylenepentamine were purchased from Sigma-Aldrich (St. Lois, MO). For each surfactant synthesis, PIB succinic anhydride (PIBSA) from Chevron Oronite (San Ramon, CA) and polyamines in a 1:1 ratio were refluxed in xylenes for 10 h using Dean-Stark to remove water, affording a mixture of major mono PIB analog and minor DiPIB analog (Scheme 1).[24] The PIB succinimide (PIB-1) was synthesized with the succinic anhydride and urea, heated without solvent. The PIB tail for each sample had the same molecular weight, ~1000 g/mol. Each product was purified by column chromatography. Two fractions were collected after separation for experimentation, one with a mono-substituted PIB tail and the other with di-substituted PIB tails to one polyamine head (Scheme 1). The structure of PIBSA was based on the fact that such products are often obtained by an Alder-ene reaction.[24-26] These synthesized surfactants are referred to as PIB-1 through PIB-5, representing the mono-substituted PIB tail and polyamine number, and DiPIB-2 through DiPIB-5, representing the di-substituted PIB tails and polyamine number. The products were verified with FTIR and CHN elemental analysis.

PIB succinimide polyamine is available commercially as OLOA and is commonly used in studies of charge in non-polar media.[8-13] The exact number of repeating units in the PIB tail and polyamine head of the proprietary material are not known and may vary depending on the specific OLOA version. The OLOA 371, 1200, and 11000 are all cited as similar PIB succinimide surfactants,[11,27] but there is disagreement whether they contain a pentamine[28] or triamine[29] and have different assumed molecular weights of 1700 g/mol[27], 1200 g/mol[9], and 950 g/mol[30] with high polydispersity[21,23]. The OLOA 371 and 1200 versions come diluted in 50% mineral oil and studies that attempt to de-oil the material find irreproducibilities.[9,10,29] The OLOA 11000 is a concentrated version of OLOA 371[31], up to 72% active component[13], versus 50%. Morrison describes the possible number of reaction products in OLOA synthesis as being “manifold”.[5] Such factors could effect charge stabilization in non-polar solutions.

For comparison with the synthesized samples, we also considered the commercially available PIB succinimide polyamine surfactant OLOA 11000 and PIB succinic anhydride OLOA 15500 from Chevron Oronite. These will now be referred to as O11k and PIB-0, respectively. The structures of new surfactants studied are shown in Scheme 2. The DiPIB-3 is shown as an example the di-substituted tail by-product, which was present in each synthesis of PIB-2 through PIB-5 and separated through column chromatography. Molecular weight of the PIB tail is ~1000 g/mol.

All surfactant samples were prepared to 3 wt%, well above the critical micelle concentration[23], in isoparaffinic fluid from ExxonMobil (Irving, TX). Sonication for 20 min in a bath sonicator ensured dissolution.

Scheme 1 Synthesis of Dispersants from PIBSA and Polyamine

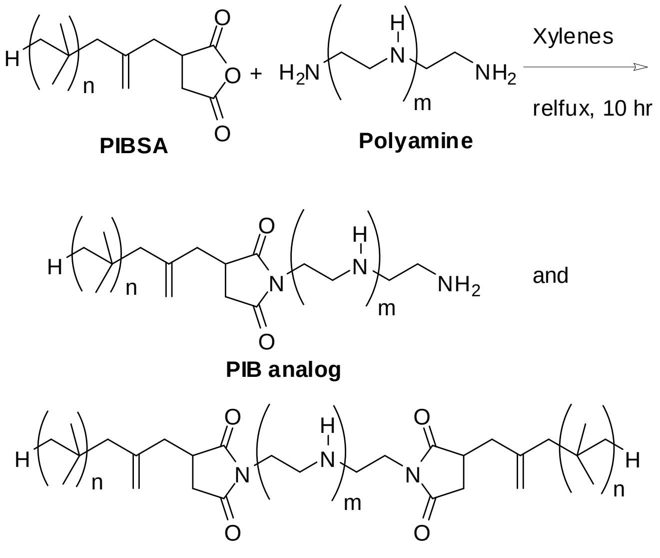

Scheme 2 Dispersants Studied

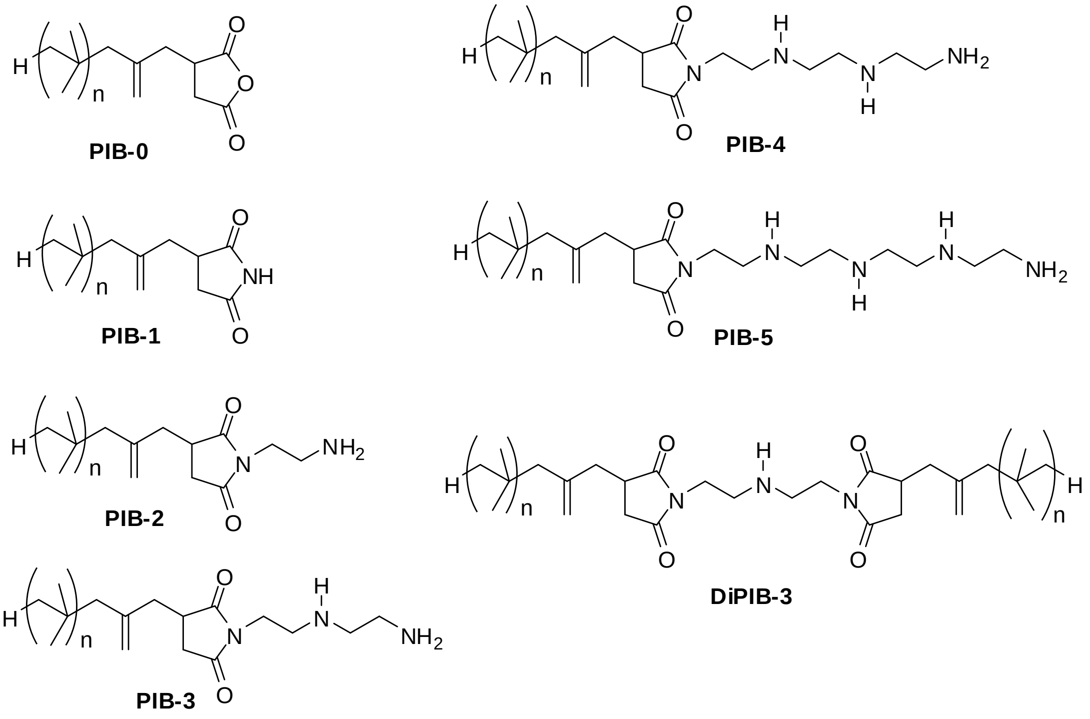

2.2. Scattering techniques. Small-angle x-ray scattering (SAXS) was conducted at the Stanford Synchrotron Radiation Lightsource on beam line 1-4. Surfactant samples were loaded into 1 mm thick sample holders with Kapton polyimide film windows (DuPont, Wilmington, DE). The range in scattering vector (q) was 0.1–5.5 nm^{-1}. The detector distance and beam center were calibrated with a silver behenate standard sample. Exposure times were 5 min. Dark and solvent-only scattering were determined with no beam and solvent-only sample holders and used for background subtraction. The data were modeled using the Irena[32] macros package for Igor Pro using NIST form factors[33]. Electron density contrast parameters for the model were determined in Irena by inputting the molecular formulas and chemical mass densities.

Dynamic light scattering (DLS) measurements were conducted on a Zetasizer Nano ZS (Malvern, Worcestershire, UK) fitted with a 633 nm laser and a 173^{o} detector scattering angle. The solvent viscosity was input as 1.29 cP, the solvent refractive index as 1.43, and the PIB surfactant refractive index as 1.59. Using these input values, Zetasizer algorithms determine a diffusion coefficient from the decay rate of the correlation function of a sample's scattering intensity differences over time and then a size from the Einstein-Stokes relation. The DLS results are given with error bars for the average of 4 measurements.

2.3. Transient current. Parallel plate cells with geometry of 0.5 cm^2 × 10 μm were used to test the surfactant samples. The electrode materials were gold on glass and indium tin oxide (ITO) on polyethylene terephthalate (PET). The ITO was patterned with a square grid of epoxy-based negative photoresist (SU-8) walls to define the 10 μm cell height. Voltages were applied (TREK power amplifier, Medina, NY) and resulting current signals were recorded (Stanford Research Systems low-noise current preamplifier, Sunnyvale, CA) through LabView (National Instruments, Austin, TX).

For charge concentration measurement, the applied voltage waveform was +100 V for x seconds, 0 V for 4 s, -100 V for x seconds, and 0 V for 4 s. The pulse time x was varied from 0.0007 s to 0.1 s. The 0.1 s case for PIB-3 is shown in Figure 1. While the voltage is applied, the cell becomes polarized and the charged micelles migrate and collect at the electrodes. This is shown from 0-0.1 s and 4.1-4.2 s in Figure 2. When the voltage is turned off a reverse transient current peak is formed, as seen in Figure 2 from 0.1-4.1 s and 4.2-8.2 s, due to the gradual release of the charges back into the bulk solution[13]. Integration of this reverse transient, accounting for the cell geometry, gives the charge concentration of the system. Charge concentrations are given with error bars for 6–9 transient current measurements averaged together.

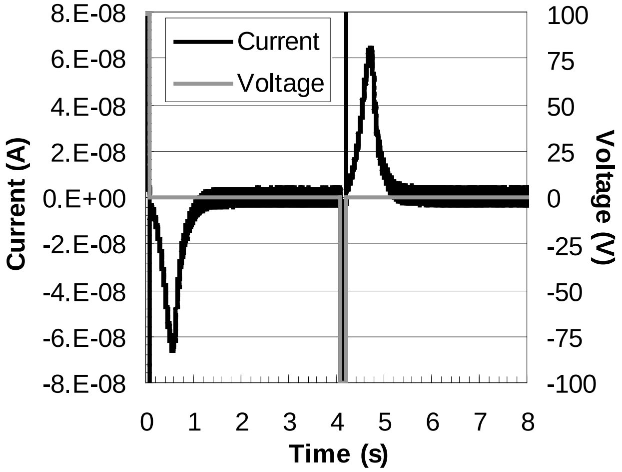

Figure 1. An example of a transient current experiment for PIB-3 with 0.1 s 100 V pulses. Voltage is shown in the grey line and current in black.

For conductivity measurements, a smaller applied voltage (0.5-10 V) was pulsed and the forward transient current was recorded for the first ~10 milliseconds. The conductivity is found by extrapolating the current to time zero to determine the initial current while accounting for the applied voltage and cell geometry.

2.4. Application to electrophoretic inks. After characterizing the surfactant-only solutions, inks were formulated to study the effects on device performance. Surfactant solutions were first formulated as described above. Then magenta pigment particles were added to 1.5 wt% and sonicated for 2 h in a bath sonicator to ensure dispersion. To avoid over-heating, the sample was removed from the sonicator for cool-down time after 1 h of sonication before completing the final hour of sonication.

To measure colorant particle size, each sample was diluted 1:30 in the solvent to reduce attenuation of the incident light by the particles. Zeta potential of the magenta particles was also measured with the Zetasizer with the fluid diluted 1:30. A dip cell with 2 mm palladium electrodes was submerged into the sample and the applied voltage was set to 40 V. The dip cell was washed between samples by rinsing in the isoparaffin solvent, sonicating in the solvent for 5 min, rinsing with the solvent, and drying with air. The Zetasizer ran both slow and fast field reversals and used the Huckel approximation to calculate the zeta potential from the mobility measured from the phase analysis light scattering. The dispersant dielectric constant was input as 2. Zeta potentials here are presented with error bars for the average of 3 measurements.

The test device used to evaluate electrophoretic ink performance had interdigitated ITO electrodes on glass and a PET cover patterned with square grids of SU-8 walls to define the cell height. Applied voltage (Agilent power supply, Santa Clara, CA) was switched to +20 V and -20 V and transmitted light microscopy videos (Leitz Metallux 3, Wetzlar Germany) of the device were recorded through Windows Movie Maker.

3. Results and Discussion

3.1. Micelle size. For SAXS, the intensity *I(q)* results were modeled using Equation 1, where *N* is a fitting parameter proportional to the micelle concentration. Form factors for both a sphere and for a core-shell sphere were used from NIST.[33] Attempts at modeling the micelles as cylinders or spheroids (ellipsoids of revolution) matched poorly with the data, suggesting the micelles were indeed spherical. The form factor for a core-shell particle is shown by *P(q)* in Equation 2. The sphere form factor simply neglects the first two terms. The subscripts represent the core *C* and the shell *S* (or the whole sphere *S* in the non-core-shell case). The radius and volume are given by *r* and *V*, and ρ is electron density.

$$I(q) = NP(q) \qquad (1)$$

$$P(q) = V_C{}^2(\rho_C - \rho_S)^2 F_C{}^2 + 2V_C V_S(\rho_C - \rho_S)(\rho_S - \rho_{solvent})F_C F_S + V_S{}^2(\rho_S - \rho_{solvent})^2 F_S{}^2 \qquad (2)$$

$$F_x = \frac{3\left(\sin(qr_x) - qr\cos(qr_x)\right)}{\left(qr_x\right)^3} \tag{3}$$

The electron density contrast $\Delta\rho$ is the electron density difference between the micelle and solvent molecules. The core-shell model took into account the (small) electron density difference between the micelle core and micelle shell as well as that between the micelle shell and the solvent. Assuming an amine core and a PIBS shell, the following values were input into the model fits for ρ in units of 10^{10} cm^{-2}- core = 9.16, shell = 8.80, and solvent = 7.42. Figure 2 shows the fit of both models to the data. Both fit the data well, but the core-shell model is slightly better at the highest *q*, which represents length scales on the order of 1 nm. Table 1 shows the SAXS micelle size results in the first three columns.

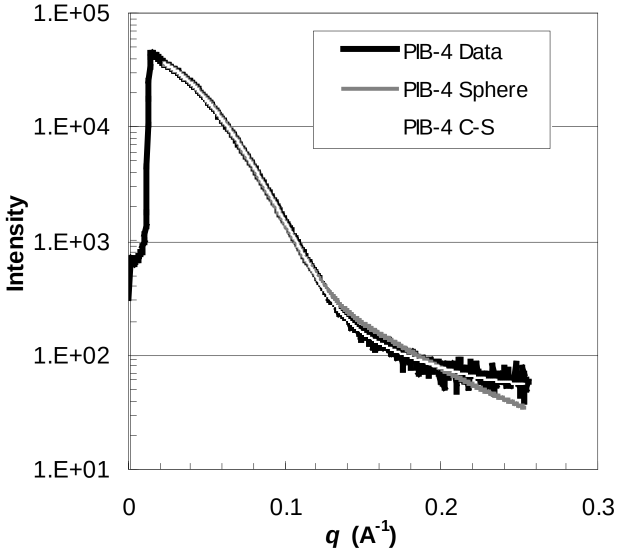

Figure 2. Example of the sphere model (grey) and the core-shell model (white) compared to the SAXS data (black) for PIB-4. Both models fit the data well, with the core-shell model matching only slightly more closely at larger *q*.

Table 1. Micelle Diameter (nm) from Sphere and Core-Shell SAXS Models and DLS Data

	Sphere	C+S	Core	DLS
PIB-2	4.7	4.5	2.6	10.4
O11k	5.3	5.3	5.3	11.3
PIB-3	5.6	5.6	4.6	164
PIB-4	7.1	7.2	4.7	13.4
PIB-5	7.9	7.8	3.7	15.5
DiPIB-2	3.2	3.2	3.2	8.4
DiPIB-4	4.0	3.9	2.6	8.4
DiPIB-5	3.1	3.2	2.5	7.0

Since the electron density contrast is small for the shell-core compared to both the solvent-core and solvent-shell, the SAXS is primarily sensitive to the diameter of the core plus shell. This is evident in Table 1, which shows the best fit sphere diameters are close to the core-plus-shell diameters. Similarly, the core-shell contrast is too small to resolve the shell, so the shell thickness values are not reliable. It is expected that there is a gradual change in the electron density from that of the PIB tails closest to the core to that of the solvent at the tail ends. Therefore, it is likely the SAXS diameter results are an underestimation of the actual core-plus-shell size. Regardless, the results show that increasing the polyamines increase the micelle size. The O11k most closely matches the PIB-3 size. Di-substitution of the PIB tail decreases the micelle size, which is expected due to increased steric hindrance causing more curvature[7,34].

The DLS measurements accessed the core-plus-shell diameters plus the associated solvent bound to the micelles since it is a measurement of hydrodynamic radius and includes the solvation effects. The same trends as SAXS emerge (Table 1). Increasing polyamines increase the micelle size, O11k falls in between PIB-2 and PIB-4, and di-substitution of the PIB tail decreases the micelle size. Interestingly, PIB-3 does not follow trend in the DLS results, perhaps due to an increased affinity for aggregation.

3.2. Transient current. To determine the effect of surfactant head group chemistry on charge stabilization, transient currents were measured. Figure 3A shows samples PIB-0 through PIB-5 have increasing charge concentration as polyamine number increases. This indicates that more amines in the polar head give an increased capability for the micelles to stabilize charge in the non-polar solvent. Similarly, Figure 3B compares the charge concentration for samples of PIB-3 containing various fractions of its double-tailed analog DiPIB-3. This double-tailed version is a by-product of the synthesis reaction for each of the single-tailed PIB-amines, which we separated out. The PIB-3 and DiPIB-3 surfactants were chosen for this comparison since O11k behaved most like PIB-3 in size and transient current experiments, and it likely contains a mixture of the mono-substituted and di-substituted versions. At a 5% DiPIB fraction, there is not a significant effect on charge. The reaction procedure we used to synthesize the PIB surfactants did not produce more than 5% DiPIB so it was perhaps unnecessary to remove this insignificant fraction from our samples. The O11k had lower charge stabilization capability than the 5% DiPIB synthesized sample. Based on the linear trend for decreasing charge concentration with increasing DiPIB, O11k data falls at ~16% DiPIB fraction. This suggests that either the O11k manufacturing procedure uses different conditions that enrich the double-tailed fraction, or there is something else in O11k that is lowering the concentration of charge generating ions. Additionally, it is interesting to see that 100% DiPIB samples have essentially zero charge concentration, suggesting that the micelles are too small (Table 1) to effectively stabilize charge in the non-polar solvent.

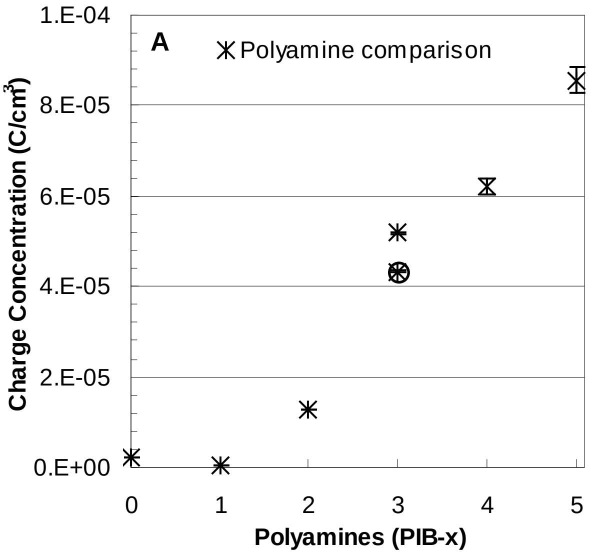

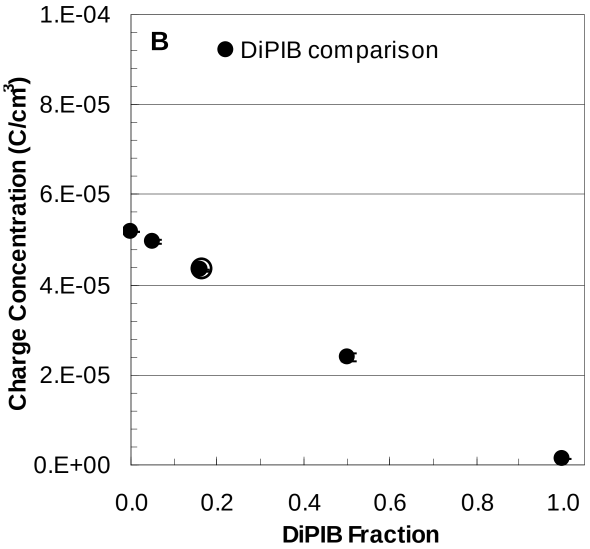

Figure 3. The charge concentration measurements for the different surfactant solutions with varying polyamine head groups (A, stars) and for different mixtures of PIB-3 with DiPIB-3 and O11k (B, filled circles). The O11k data are indicated with outlined markers.

In addition to measuring the charge stabilization capability of the micelles, the transient current method also determines a hydrodynamic size for the micelles. The experiments collect both charge concentration data (ρ_q), as well as solution conductivity (σ), which is based on initial current. Therefore, mobility μ is calculated (Equation 4) and micelle size (radius r) can be determined from the Einstein-Stokes relation (Equation 5). The solution viscosity is η, and we assume a univalent charge per micelle, where q is the charge of a single electron.

$$\mu = \frac{\sigma}{\rho_q} \tag{4}$$

$$\frac{\mu k_B T}{q} = \frac{k_B T}{6\pi\eta r} \tag{5}$$

Figure 4 shows a comparison of the different size measurements. The transient current method is in good agreement with DLS, which is to be expected since both are measuring the hydrodynamic radius of the micelle. The transient current method is less accurate for samples that have low charge, as with

PIB-0 and PIB-1. The SAXS and DLS measurements have a consistent difference of ~6 nm for each sample, which represents the associated bound solvent and PIB tail portions that are underestimated in SAXS as discussed in Section 3.1.

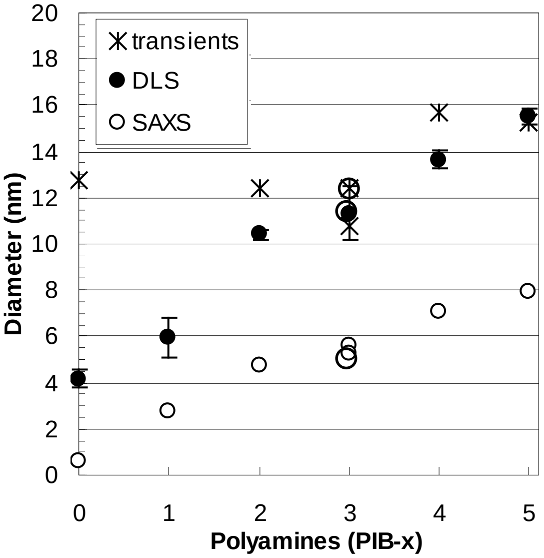

Figure 4. Comparison of the various sizing methods- SAXS (empty circles), DLS (filled circles), and the calculated diameter based on transient current measurements (stars). The *x*-axis represents each of the five synthesized surfactants as well as the PIB succinic acid at *x* = 0 and O11k at *x* = 3 in outlined markers.

The Bjerrum length for a non-polar medium is ~28 nm as discussed in the introduction, but the presence of surfactants reduces λ_B through stronger screening by the polar polyamine head groups. We show evidence that more polyamines increase the charge concentration (Figure 3A) as well as micelle size (Figure 4). The effect of increasing polyamines on the size and charge needs to be decoupled through further experiments with synthesized surfactants of similar head length but varying chemistries. One step towards this decoupling is the comparison between PIB-0 and PIB-1 charge. Both have low charge and similar molecular size, but different chemistries (succinic anhydride versus succinimide, respectively). This is initial evidence that polar head size (micelle size) dominates the charge concentration rather than head group chemistry. Considering larger head group sizes with differing chemistries will give more information about the charge concentration trends with surfactant head size and chemistry.

3.3. Electrophoretic inks. The understanding of micelle characteristics (e.g., size) on charge concentration in non-polar solutions that we have obtained will give insights into improving electrophoretic ink performance. To this end, magenta dispersions were formulated with each of the PIB surfactants and voltages were applied to test devices with the inks. Ideally, the colorant should migrate to and compact onto the electrodes to enable a “clear-state” in the device. Figure 5 shows examples of four of these test devices with voltage applied. The negative and positive bars indicate the position of two of the interdigitated electrodes. The PIB-1 sample does not make a good dispersion (poor contrast), while the other surfactants do, suggesting an amine in the polar head is necessary for colorant particle stabilization. Polyamines of PIB-3 or greater show similar acceptable compaction to the electrodes.

The poor dispersion of the PIB-1 formulated ink is also evident in the colorant particle size measurements. All the dispersions averaged 290 nm particle size, except for the PIB-1 sample, which was 1340 nm, indicating significant particle aggregation. Another indicator of particle stability is zeta potential, which is the electric potential at a suspended particle’s slipping plane and thus representative of particle-particle repulsion.[35] The zeta potential of the PIB-1 sample was 20 mV, which was 20-40 mV lower than the other samples. These values are shown in Figure 6, along with the corresponding surfactant-only samples’ charge concentrations.

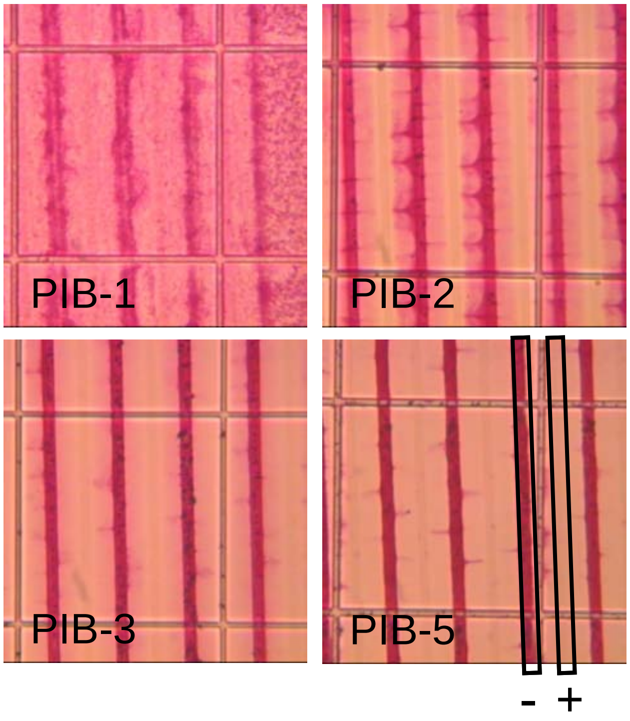

Figure 5. Test devices of magenta colorant with various synthesized surfactants under applied voltage. The bottom-right image shows approximately where two of the interdigitated electrodes are. PIB-4 is not shown since it was similar to PIB-3 and PIB-5.

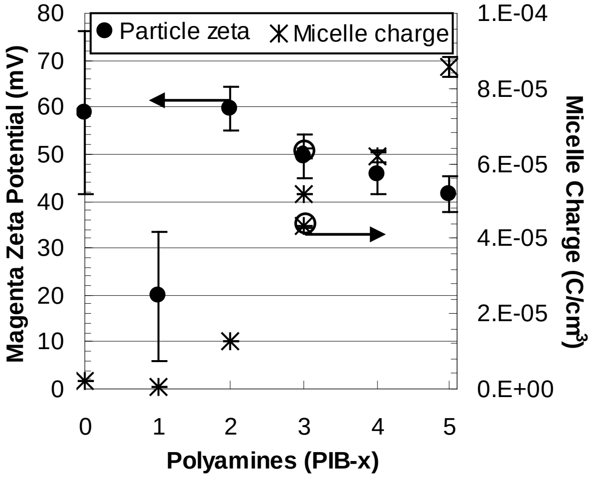

Figure 6. Particle zeta potential (filled circles) and the surfactant-only solution charge concentration (stars) for samples made with PIB-1 through PIB-5 as well as O11k in outlined markers.

For the inks that are properly dispersed, there appears to be an inverse relationship between the surfactant-only charge concentration and the colorant particle zeta potential. A few studies show results where increasing surfactant concentration in non-polar solvents decreases particle charge[16,17], which is analogous to our results assuming increasing surfactant concentration increases charge stabilization capability. However, some authors report the opposite trend[9,10], while others find zeta potential is insensitive to surfactant concentration in non-polar solvents[22]. These differences in the literature may be reconciled by considering the surfactant concentration regime of the experiments. Studies investigating over five orders of magnitude of different surfactant concentrations show there are three regions of different zeta potential behavior depending on surfactant concentration.[15,18,23] Below the critical micelle concentration, particle zeta potentials are low and constant until micelles can form and stabilize charge, after which there is a sharp increase in zeta potential. Then, at high surfactant concentrations, the zeta potential decreases for reasons that are not well understood.

Our experiments were conducted at a high surfactant concentration and small chemistry differences in the surfactant polar head group had a large effect on increasing charge stabilization. Several studies hypothesize that there is particle charge neutralization at high surfactant concentrations in non-polar media resulting from adsorption of charged species in the fluid onto the particle surface.[15,23] However our system contained only nonionic surfactants. Another explanation is that charge screening plays a role in particle zeta potential in non-polar dispersions. In polar solutions it is common to see decreased zeta potential with increased ion concentration due to increased charge screening. Whether the same screening effect applies to non-polar solutions is unclear since there is only a small number of micelle charge directors present to decrease the electric double layer compared to ions in aqueous solutions.[5] However, more recent analysis shows constant particle surface potential with decreasing mobility in non-polar suspensions[16], suggesting charged reverse micelles can effectively screen. It has been our experience that it is difficult to make general correlations between non-polar charge concentration and particle zeta potential. For example, PIB-0, which gave a charge concentration an order of magnitude smaller than PIB-2, made a magenta ink with a zeta potential equal to the PIB-2 sample (Figure 6). Interpretations need to be made on a case by case basis and take into account surfactant chemistry differences, for example the presence of an anhydride, imide, or amine in the polar head could affect electrophoretic ink performance differently.

4. Conclusions

In this study we have used three techniques to access micelle size: SAXS gives the micelle core plus an underestimated shell, while DLS and transient current measurements provide the micelle hydrodynamic radius. Both micelle size and charge increase with increasing polyamines used for the polar head. Whether it is specifically the polyamines or the size that are causing the increased charge stabilization remains to be decoupled, but these initial results suggest that polar head size dominates the stabilization effect. Commercial O11k behaves like PIB-3 suggesting it contains a triamine polar head, but likely with di-substituted by-products or a lower concentration of charge generating ions, since there are charge stabilization differences. Extending the surfactant variations to electrophoretic ink performance showed that the triamine polar head was sufficient for acceptable device performance while the absence of amine made a poor dispersion. It is concluded that correlations between the charge concentrations of surfactant-only solutions with electrophoretic ink performance need take into account surfactant chemistry differences. The presence of an anhydride, imide, or amine in the polar head group affects electrophoretic ink performance differently, as well as even smaller chemistry differences, such as the just the number of amines present.

Acknowledgements

This material is based upon work supported by the National Science Foundation under Grant # EEC-0946373 to the American Society for Engineering Education. Portions of this research were carried out at the Stanford Synchrotron Radiation Lightsource, a Directorate of SLAC National Accelerator Laboratory and an Office of Science User Facility operated for the U.S. Department of Energy Office of Science by Stanford University. The authors thank John Pople at SSRL and Josh Cuppett for assistance with SAXS measurements on beam line 1-4 and Ana Morfesis at Malvern for assistance with Zetasizer measurements.

References

1. Ota, I.; Ohnishi, J.; Yoshiyama, M. *Proc. IEEE* **1973,** *61,* 832.
2. Comiskey, B.; Albert, J. D.; Yoshizwa, H.; Jacobson, J. *Nature* **1998,** *394*, 253.
3. Jones, S. A.; Martin, G. P.; Brown, M. B. *J. Pharm. Sci.* **2006,** *95,* 1060.
4. Rosenholm, J. B. *Colloids Surf., A* **2010,** 354, 197.
5. Morrison, I. D. *Colloids Surf., A* **1993,** *71,* 1.
6. Eicke, H. F. In *Topics in Current Chemistry*; Springer: Berlin, 1980; Vol. 87, Chapter 2, p 85.
7. Luisi, P. L.; Magid, L. J. *Crit. Rev. Biochem. Mol. Biol.* **1986,** *20,* 409.
8. Murau, P.; Singer, B. *J. Appl. Phys.* **1978,** *49,* 4820.
9. Fowkes, F. M.; Pugh, R. J. *ACS Symp. Ser.* **1984,** *240,* 331.
10. Kornbrekke, R. E.; Morrison, I. D.; Oja, T. *Langmuir* **1992,** *8,* 1211.
11. Strubbe, F.; Verschueren, A. R. M.; Schlangen, L. J. M.; Beunis, F.; Neyts, K. *J. Colloid Interface Sci.* **2006,** *300,* 396.
12. Prieve, D. C.; Hoggard, J. D.; Fu, R.; Sides, P. J.; Bethea, R. *Langmuir* **2008,** *24,* 1120.
13. Kornilovitch, P.; Jeon, Y. *J. Appl. Phys.* **2011,** *109,* 064509.
14. Novotny, V; Hopper, M. A. *J. Electrochem. Soc.* **1979,** *126,* 925.
15. Keir, R. I.; Suparno, Thomas, J. C. *Langmuir* **2002,** *18,* 1463.
16. Hsu, M. F.; Dufresne, E. R.; Weitz, D. A. *Langmuir* **2005,** *21,* 4881.
17. Smith, P. J., Jr.; Patel, M. N.; Kim, J.; Milner, T. E.; Johnston, K. P. *J. Phys. Chem. C* **2007,** *111,* 840.
18. Sainis, S. K.; Merrill, J. W.; Dufresne, E. R. *Langmuir* **2008,** *24,* 13334.
19. Guo, Q.; Singh, V.; Behrens, S. H. *Langmuir* **2010,** *26,* 3203.
20. Espinosa, C. E.; Guo, Q.; Singh, V.; Behrens, S. H. *Langmuir* **2010,** *26,* 16941.
21. Sainis, S. K.; Germain, V.; Mejean, C. O.; Dufresne, E. R. *Langmuir* **2008,** *24,* 1160.

22. Roberts, G. S.; Sanchez, R.; Kemp, R.; Wood, T.; Bartlett, P. *Langmuir* **2008,** *24*, 6530.
23. Poovarodom, S.; Berg, J. C. *J. Colloid Interface Sci.* **2010,** *346,* 370.
24. Shen, Y.; Duhamel, J. *Langmuir* **2008,** *24,* 10665.
25. Walch, E.; Gaymans, R. J. *Polymer*, **1994**, 35, 1774.
26. Pucci, A.; Barsocchi, C.; Rausa, R.; D'Elia, L.; Ciardelli, F. *Polymer*, **2005**, 46, 1497.
27. Kim, J.; Anderson, J. L.; Garoff, S.; Schlangen, L. J. M. *Langmuir* **2005,** *21*, 8620.
28. Qi, D. M.; Bao, Y. Z.; Weng, Z. X.; Huang, Z. M. *Polymer* **2006,** *47,* 4622.
29. Al-Ghamdi, G. H.; Sudol, E. D.; Dimonie, V. L.; El-Aasser, M. S. *J. Appl. Polym. Sci.* **2006,** *101*, 3479.
30. Barz, D. P. J.; Vogel, M. J.; Steen, P. H. *Langmuir* **2010,** *26*, 3126.
31. Tynik, R. J.; Donnelly, S. G.; Aguilar, G. A. U.S. Patent Appl. US 2007/0203033 A1, 2007.
32. Ilavsky, J.; Jemian, P. R. *J. Appl. Cryst.* **2009,** *42,* 347.
33. Kline, S. R. *J. Appl. Cryst.* **2006,** *39,* 895.
34. Shrestha, L. K.; Sato, T.; Dulle, M.; Glatter, O.; Aramaki, K. *J. Phys. Chem. B* **2010,** *114,* 12008.
35. Delgado, A. V.; Gonzalez-Caballero, F.; Hunter, R. J.; Koopal, L. K.; Lyklema, J. *Pure Appl. Chem.* **2005,** *77*, 1753.